DELIVERABLE REPORT

WP9 JRA4 – Research on Time-resolved ultrafast probes on nanosystems

D9.3

Demonstration of a multiple beam delay line for X-ray streaking experiments

Expected date

M36

NFFA-Europe has received funding from the EU's H2020 framework programme for research and innovation under grant agreement n. 654360

nffa.eu

PROJECT DETAILS

PROJECT ACRONYM	PROJECT TITLE
NFFA-Europe	NANOSCIENCE FOUNDRIES AND FINE ANALYSIS - EUROPE
GRANT AGREEMENT NO:	FUNDING SCHEME
654360	RIA - Research and Innovation action
START DATE	
01/09/2015	

WP DETAILS

WORK PACKAGE ID	WORK PACKAGE TITLE
WP9	JRA4 – Research on Time-resolved ultrafast probes on nanosystems

WORK PACKAGE LEADER

Dr. Emmanuel Stratakis (FORTH)

DELIVERABLE DETAILS

DELIVERABLE ID	DELIVERABLE TITLE
D9.3	Demonstration of a multiple beam delay line for X-ray streaking experiments

DELIVERABLE DESCRIPTION

Demonstration of a multiple beam delay line for X-ray streaking experiments

EXPECTED DATE	ESTIMATED INDICATIVE PERSONMONTHS
M36 31/08/2018	MM

AUTHOR(S)

Christian David, Benedikt Rösner, Gediminas Seniutinas

PERSON RESPONSIBLE FOR THE DELIVERABLE

Emmanuel Stratakis (FORTH)

NATURE

P - Prototype

DISSEMINATION LEVEL

- ☒ P – Public
- ☐ PP - Restricted to other programme participants & EC: (Specify)
- ☐ RE - Restricted to a group (Specify)
- ☐ CO - Confidential, only for members of the consortium

nffa.eu

REPORT DETAILS

ACTUAL SUBMISSION DATE	NUMBER OF PAGES
06/09/2018 hh.mm AM	**13**

FOR MORE INFO PLEASE CONTACT

Dr. Christian David Tel. +41-56-310 3753 Email: christian.david@psi.ch

Version	Date	Author(s)	Description / Reason for modification	Status
1.0	17/06/2018	Benedikt Rösner	First draft	Draft
1.1	18/08/2018	Christian David	Revision	Revision
1.2	21/08/2018	Benedikt Rösner	Correction of Details	Final

Contents

Executive Summary

We designed and fabricated optical elements in order to streak the time delay of an incoming EUV beam along one dimension on a two-dimensional detector. This concept allows for conducting pump-probe experiments with time windows of up to 3.5 ps in a single shot from an XFEL. We tested this concept in two XFEL beamtimes at the DiProI beamline at FERMI. With this approach, we are able to investigate magnetic dynamics in scientifically and technologically relevant magnetic materials.

By tailoring the optical elements, we furthermore opened up a possibility to investigate compound materials at two different absorption edges without major changes in the experimental geometry. Two different off-axis zone plates are mounted in this case, and the energy can be easily switched forth and back from one absorption edge to the other. This is a major advantage in terms of speed and efficiency of an experiment. Taking this approach further, we have developed a dedicated optical element that can be illuminated with a beam containing two different energies in a fixed ratio. This novel off-axis zone plate additionally includes an integrated beam splitter, allowing us to separate two diffraction orders for normalization purposes.

1. Concept

The advent of femtosecond lasers has provided a powerful tool for the study of transient matter. In pump-probe experiments, they are used to push a system out of equilibrium using a pulsed excitation (pump) and the subsequent relaxation dynamics are measured by applying a second pulse to determine the status of a particular property of the sample after a given delay (probe). With the advent of suitable sources, X-ray and extreme ultraviolet (EUV) probe pulses are receiving increasing attention, as they offer many contrast mechanisms to reveal element-specific and chemical information. When using multi-keV or hard X-rays, the structural dynamics of matter can be probed by diffraction experiments [1], whereas the reflectance or transmission of samples can offer valuable insights in the soft X-ray and EUV regime [2].

Most common pump-probe experiments measure one particular delay after the arrival of the pump pulse at a time. Consequently, these techniques are essentially limited to the study of reversible processes that reproducibly return to their ground state after each pump-probe cycle, or they require an identical, fresh sample for each shot. This has hindered pump-probe studies of highly excited materials at near solid densities as they reach local thermal equilibrium: the so-called ‘‘warm dense matter’’ regime [3]. Since these very high-energy density experiments permanently damage the samples with each shot, and constant supply of fresh identical samples is only possible in some experiments, it is most useful to find a way to get complete time traces of the response from a single X-ray pump pulse. Another important limitation for ultrafast time-resolved experiments at X-ray FEL sources has been the loss in time resolution due to the timing jitter between the pump and probe pulses. Typically, the external pump lasers are synchronized to the X-ray FEL via radiofrequency phase-locking, resulting in short term jitter of more than 100 fs [4], and long term drifts in the picosecond range. The development of more advanced techniques, e.g. exploiting the terahertz emission from the FEL undulator [5] or the signal from electron bunch monitors [6] for the stabilization of the X-ray and optical pulses, is a topic of intense research. A pragmatic and robust method involves monitoring the relative time delay on a per-shot basis and re-sorting the data

accordingly. This approach can reduce timing errors to below 10 fs [7], but it obviously requires data sets collected using many pump pulses and is therefore limited use for single-shot experiments. A fundamental way to avoid timing jitter between pulses is to split them from the same parent pulse and to control their temporal separation by a delay line. Several such instruments based on mirrors [8,9] and Bragg crystals [10,11] have been developed for soft and hard X-ray FEL radiation, respectively. However, both approaches only provide one delay time per X-ray pulse.

A split-and-delay approach can be based on diffraction gratings [1], as shown in Figure 1. A set of beam splitter gratings S_n with different periods p_n diffracts a small fraction of the incoming radiation into a fan of beams. A second set of gratings R_n is positioned half way between S_n and the sample to recombine the diffracted beams with the direct, undiffracted beam at the sample position. For this purpose, the recombiner periods q_n must be half the period p_n of the corresponding S_n grating. For weakly diffracting S_n gratings, most of the intensity remains in the undiffracted beam, which can be used as a pump pulse to excite the sample. This pulse is followed by a series of probe pulses, each a diffracted beam, with delays that are precisely defined by the geometrical parameters and not subject to any pump-probe jitter. The probe beams diverge again downstream of the sample, and a streak of delayed probe pulses can be recorded on a detector array, analogously to commonly used electron streak cameras.

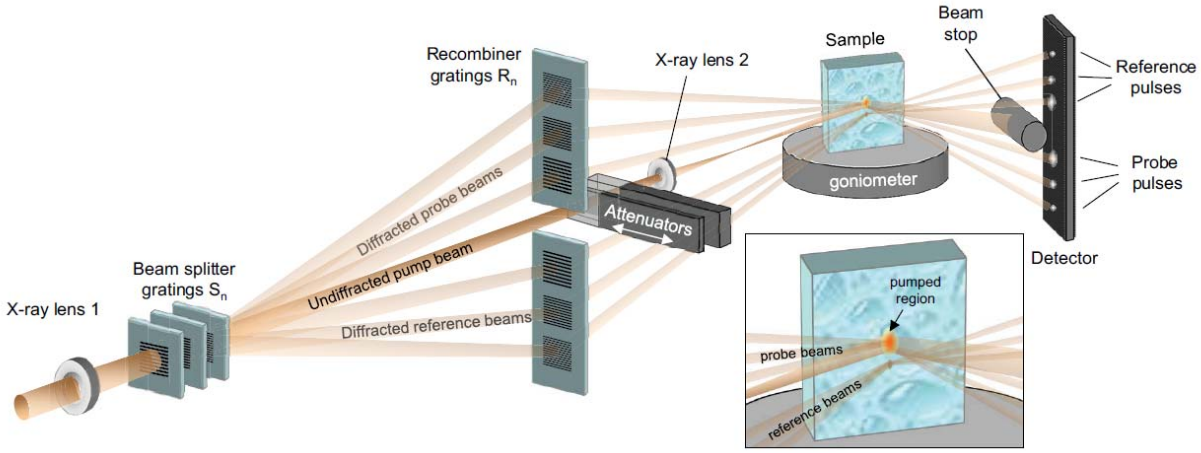

Figure 1 – The principle of X-ray streaking using diffraction gratings. Diffraction gratings are used to create a multiple split-and-delay line. The upstream lens 1 focuses the X-ray beam onto the sample. The undiffracted (direct) beam serves as a pump, and can be attenuated and focused independently by X-ray lens 2. The beams diffracted upwards by the splitter gratings S_n are redirected towards the sample by the recombiner gratings R_n, and probe the pumped sample region with defined delays. The beams diffracted downwards by S_n are steered to a region of the sample that is 100 mm below the pump beam (see inset) to provide reference signals of the unpumped response on the very same shot. All beams are recorded separately on a detector array. Only three delayed beam pairs are shown for simplicity. The sample's scattering plane is chosen perpendicular to that of the gratings, in order to minimize coupling of the scattering angles

To improve this concept further, focusing gratings – basically the outer region of a Fresnel zone plate, referred to as off-axis zone plate in the following – were used instead of multiple gratings with different periods. An off-axis zone plate has intrinsically a varying period from one side to the other, allowing for focussing the X-ray beam with different path length onto the sample [2], see Figure 2. This allows us to streak the X-ray beam continuously in time on a 2-dimensional detector, such as a

CCD camera. As the off-axis zone plate is designed in a way that the part in the beam is far from the optical axis (typically 10-30 mm), the direct beam cannot be used as pump, and the samples are pumped with an external laser.

We elaborated a scheme to investigate demagnetization dynamics in magnetic materials in transmission geometry. Probing the magnetic films with circularly polarized light in the EUV regime, demagnetization can be observed as change in transmission after pumping the magnetic layers with an infrared laser pulse. The method was tested and implemented at the DiProI beamline at FERMI. The time window observable with this method reaches up to 3.5 ps at 50 eV photon energy.

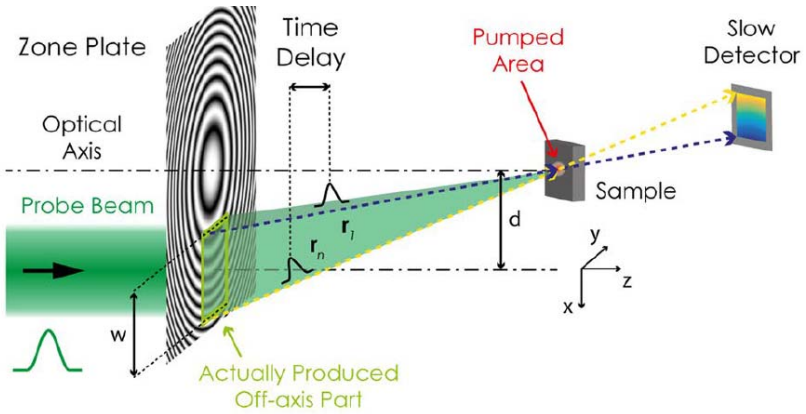

Figure 2 – The principle of X-ray streaking using an off-axis zone plate. Light travelling closer to the optical axis probes the excited area on the sample earlier than light which has been diffracted further away from it. After further propagation, the beam diverges again and is projected onto a 2-dimensional detector. The time information is then encoded on one axis of the detector whereas its resolution is then limited by the pulse length of pump and probe pulses, the number of zone pairs, and the pixel size. This allows for reconstruction of the ultrafast dynamics of the sample using a single x-ray pulse.

2. Fabrication of Optics

2.1 Design parameters of off-axis zone plates

The design of an off-axis zone plate is specified according to the experimental geometry, the beam size, the time window as a function of the number of zone pairs, and the incident energy. The principal design parameters of a conventional Fresnel zone plate, i.e. the diameter ***D***, the outermost zone width ***dr***, and its focal length at a certain energy ***E*** can be similarly found in an off-axis zone plate. The diameter of the corresponding Fresnel zone plate is expressed with the outer radius $r_o = \frac{D}{2}$. Two additional parameters define the area which is cut out of the conventional zone plate, the height $= r_o - r_i$ and the width. The radii determining the height of the optical element also define the time window, which can be calculated taking the geometry into account:

$$\Delta t = \frac{1}{c}\left(\sqrt{fl^2 + r_o^{\,2}} - \sqrt{fl^2 + r_i^{\,2}}\right),$$

with the focal length:

$$fl = \frac{D}{2 \cdot \tan\left[\arcsin\left(\frac{\lambda}{2 \cdot dr}\right)\right]}.$$

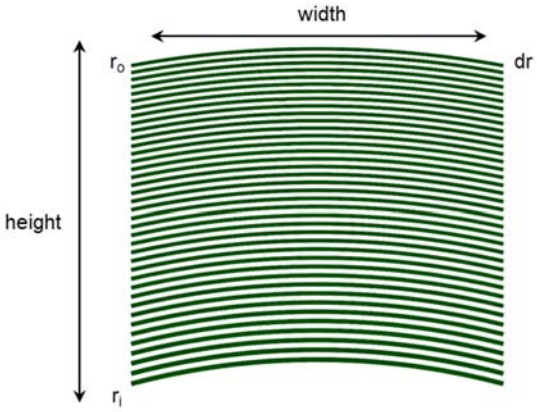

Figure 3 – Scheme of an off-axis zone plate, with its most important parameters indicated: the outer radius (r_o) corresponds to the half diameter of the Fresnel zone plate the off-axis part is cut out, the inner radius (r_i) determines the number of the innermost zone, and the area is determined by the height and the width of the optical element, whereas the height is the difference of r_o and r_i. dr is the line width of the outermost opaque zone.

We have prepared Fresnel zone plates with three different set of parameters. The first set of parameters was used at the cobalt M-edge at 60 eV. Later on, we improved our time window by the use of smaller zones, enabling to achieve a time window of 2.6 ps with a fixed focal length at both the iron M-edge (53 eV) and the nickel M-edge (66 eV). The finest zone plate (40 nm outermost zone width) can even achieve a time window of 3.5 ps at 50 eV.

- $r_o = 11.8$ mm, $r_i = 7.0$ mm, $dr = 80$ nm, width = height = 4.8 mm
  the focal length at E = 60 eV is then 80 mm, the corresponding time window 1.7 ps
- $r_o = 17.6$ mm, $r_i = 13.8$ mm, $dr = 40$ nm, width = height = 3.8 mm
  the focal length at E = 65.7 eV is then 72.6 mm, the corresponding time window 2.6 ps
- $r_o = 17.6$ mm, $r_i = 13.8$ mm, $dr = 49.9$ nm, width = height = 3.8 mm
  the focal length at E = 52.7 eV is then 72.6 mm, the corresponding time window 2.6 ps

2.2 Nanofabrication methods

Two different nanofabrication methods were applied to produce the zone plates: (i) an approach to pattern HSQ directly for the use as off-axis zone plate, and (ii) a dry etch process to etch the zone

plate structures into silicon. It should be noted that the production of 4 mm x 4 mm large optics with 40 nm line width is extremely time-demanding with electron beam lithography.

The direct patterning process is done in one lithography step. Hydrogen silsesquioxane (HSQ) is spun onto a flat, 4x4 mm large and 200 nm thick silicon membrane purchased at Norcada, Inc.. At a targeted height of 120-150 nm, the overall efficiency is reaching an optimum, slightly varying with energy. The HSQ film is then exposed in a Raith 5000+ EBPG lithography tool running at 100 kV. Typical electron doses are in the range of 12-14 mC/cm². After the exposure, which can take up to 60 hours, the nanostructures are developed in a solvent mixture AZ 351 developer and water (1:3, 5 min). The sample is then transferred into isopropanol, and dried from supercritical CO_2 in a Leica Critical Point Dryer 300. The resulting structures are shown in Figure 4 (left).

The fabrication method using a dry etching process is done in the following way. The substrates for this process are similar silicon membranes as used in the previously described process, just with a thickness of 340 nm. A thin film (60 nm) of poly methyl methacrylate (PMMA) is spun onto a 10 nm thick chromium layer which was deposited on the membrane before as a hard mask. The polymer is exposed with 100 keV electrons, now with a much smaller electron dose of 4 mC/cm². Afterwards, the resist is developed in a 7:3 mixture of isopropanol and water for 10 seconds, rinsed in isopropanol and dried at air. Subsequently, the resist is descummed with oxygen in a parallel plate etcher, before the chromium mask is etched with a mixture of chlorine gas and CO_2 for 60 seconds. After pattern transfer to the chromium layer, the resist is stripped in acetone. Special attention has to be paid to the rinsing step with isopropanol as the diligence in this step has a major impact on the subsequent silicon dry etching step. Finally, the pattern is etched into silicon in an Oxford Reactive Ion Etcher under soft conditions using a gas mixture of CHF_3 and oxygen at an RF power of 100 W. The ideal etching depth is 200 – 240 nm. As last step, the chromium mask is removed in another etch step including chlorine gas (Figure 4, right).

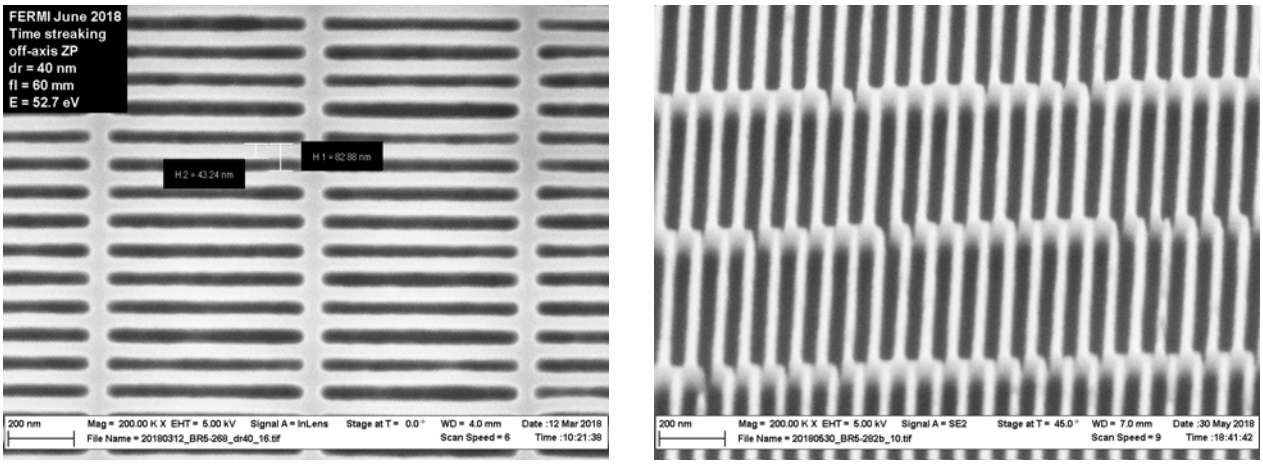

Figure 4 – SEM images of the zone plate structures. Left: 40 nm wide lines directly patterned from HSQ. Right: 40 nm wide structures etched 180 nm deep into a 340 nm silicon membrane.

2.3 Advanced optics for time-streaking experiments

A fundamental question in element-sensitive pump-probe experiments is whether a compound material of two different elements exhibits similar dynamcis for each of the contained elements. Whereas the relative dynamics in both materials can be oberserved in individual pump-probe experiments, the absolute relation in the timing of pump and probe beams is experimentally hard to achieve, if not impossible for different energies. We therefore designed an optical element which works at two specific energies.

For this purpose, we took advantage of the wealth of possiblities for shaping an EUV or X-ray beam that diffractive optics offer. We placed two off-axis zone plates next to each other in a way, that their optical axes are identical (see Figure 5, right, green and orange patterns). The parameters of the zone plates have been chosen to result in the same focal length for two specific energies, or more general for two arbitrary energies which have the same ratio: $\frac{E_1}{E_2} \approx \frac{dr_1}{dr_2}$. Figure 5 (left) shows the situation in the focal plane. When such a two-component optical element is irradiated with the two chosen energies, they will focus both energies at the same spot. As side product, the lower energy at the finer grating will be diffracted in a higher angle, whereas the higher energy at the coarser grating will be diffracted in a smaller angle. The horizontal separation in Figure 5 depicts this, showing a bright spot in the middle where both energies are in focus, and two parasitic, unfocused areas left and right from the focal spots.

For normalization purpose, the diverging, negative diffraction order of the off-axis zone plate is commonly used. However, the diverging diffraction of the two energies cannot be separated in this situation. We thus combined the off-axis zone plate with a beam splitter grating perpendicular to it by inverting the zone pairs in a regular periodicity. This approach additionally splits up the diffraction spots described before in vertical direction to equal ammounts. By the inversion of the pattern, an ideal phase grating is created, and the 0^{th} diffraction order in vertical direction is completely suppressed (which would be at Detector y = 0 mm in the ray tracing image). This allows for pumping one of the two focused spots, and taking the other spot as umpumped reference.

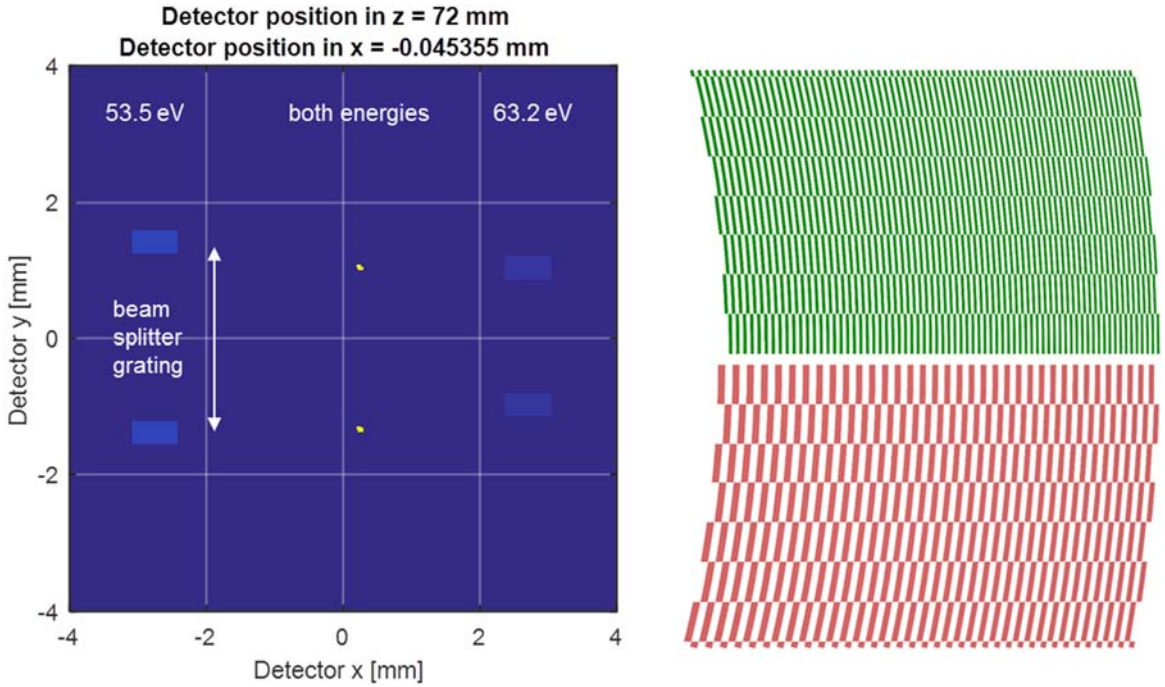

Figure 5 – Combined off-axis zone plate and beam splitter grating for two different energies (right). Left: the calculated detector image shows the traces of the EUV radiation in the focal plane when the optical element is irradiated with two light of two colours in a pre-defined energy ratio.

3. Time-Streaking Experiments

3.1 Demagnetization of cobalt films

Applying the previously described concept, a whole pump-probe experiment can be performed at once without changing the timing between pump and probe. In an experiment conducted at FERMI, we investigated the demagnetization dynamics in alloys of cobalt and dysprosium. Figure 6 shows the normalized images of the two-dimensional CCD detector, which represent the transmitted intensity through a $Co_{76}Dy_{24}$ film in a 250 mT strong magnetic field and excited by a laser pulse of 100 µJ. The two images show the comparison of an average of 500 shots (a), and a single FEL pulse (b). The time-dispersive axis is in the horizontal direction, with increasing time delay from the right to the left side. On both pictures, we can clearly see the pumping effect, even if the effect is less visible for the single shot. Those two pictures have been normalized to the unpumped intensity. We can then average the images along the direction perpendicular to the time delay (parallel to the curve in Figure 6). The resulting dynamics are shown in Figure 6 (c) as a function of time delay. In this graph, we can clearly see that the single shot signal, even if more noisy, gives the same trend as the signal obtained when we accumulate for 500 shots. This clearly demonstrates the capabilities of the X-ray streaking technique.

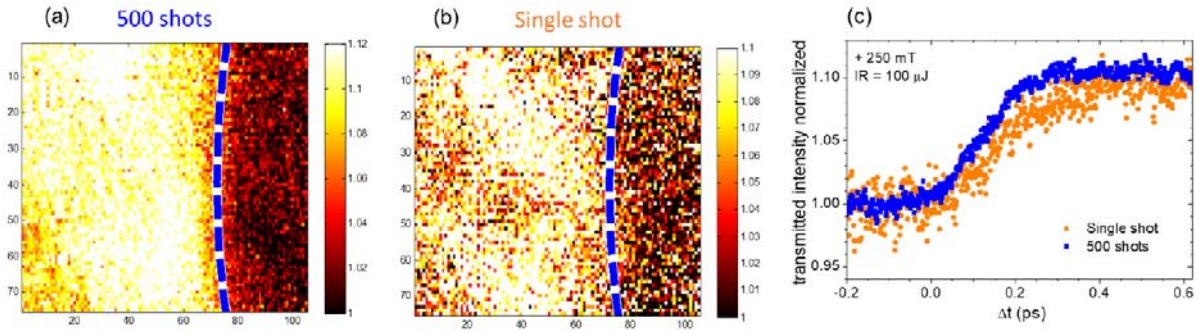

Figure 6 – XMCD signal change in transmission upon pumping a magnetic film with an IR laser. (a) Average image of 500 shots, (b) similar detector image for one single shot, and (c) time-dependent transmission change as averaged perpendicular to the time-dispersive direction as indicated with the blue line in (a) and (b).

With this concept, we conducted a systematic study on the demagnetization dynamics in different alloys and under different pump fluences (Figure 7). With that, we can show that the demagnetization time is independent of the pump fluence, but dependent on the film composition. With this geometry, we can perform systematic studies of different materials and under various conditions. A publication on this experiment is currently prepared.

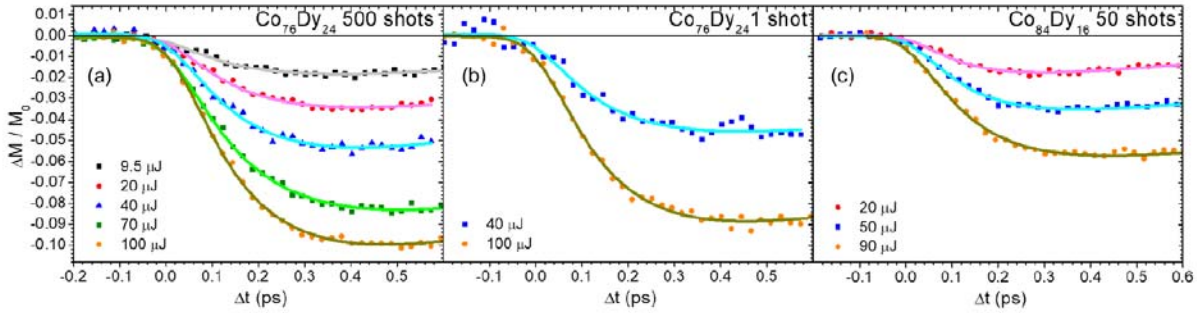

Figure 7 – Demagnetization dynamics of different alloys und different pump fluences. (a) $Co_{76}Dy_{24}$, 500 shots, 9.5 – 100 µJ pulse energy; (b) $Co_{76}Dy_{24}$, 1 shot, 40 and 100 µJ pulse energy; (c) $Co_{84}Dy_{16}$, 50 shots, 20, 50 and 90 µJ pulse energy.

3.2 Demagnetization of iron-nickel films at two energies

To investigate multicomponent films at two different absorption edges in a fixed geometry, we prepared a set of zone plates with the same focal length (and thus the same time window) for two pre-defined photon energies (see Section 2.1). This allows to switch forth and back between, for instance the nickel and the iron edge without major changes to the experimental geometry, and avoids therefore to break the vacuum during an experiment. This solution was now implemented for the investigation of permalloy and other mixed-layer iron and nickel samples in an experiment at the DiProI beamline at FERMI in June 2018. It turned out that the whole energy range between 50 and 70 eV is accessible using only two different off-axis zone plates. Furthermore, we were able to extend the time window covered with the off-axis zone plates at both absorption edges to values as high as 2.6 ps in excellent data quality as shown in Figure 8. Detailed analysis of the acquired data is currently ongoing.

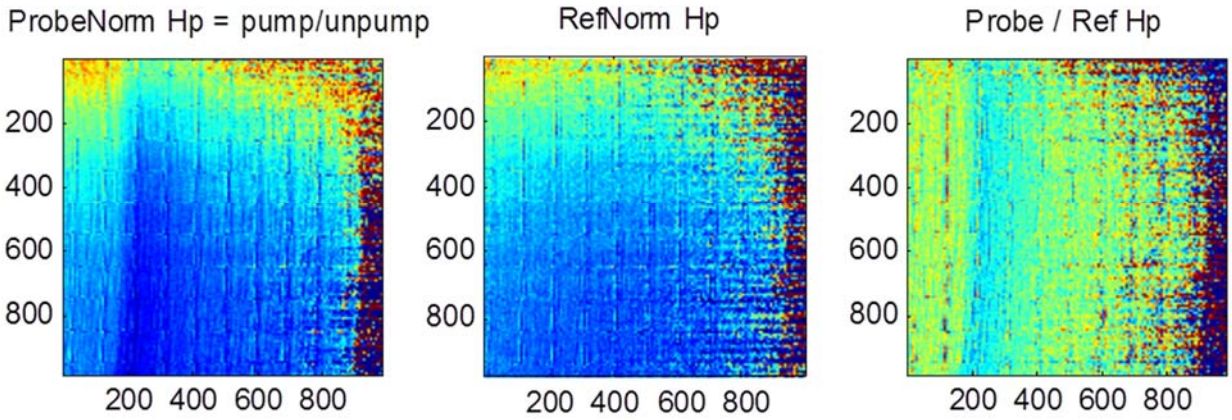

Figure 8 – Demagnetization of a permalloy film. Left: Image on the probe CCD camera. Middle: Image from the reference camera. Right: Divided image, showing the transmission change. The scale is in pixels; each pixel has a time delay of 28 fs, giving a whole time window of 2.6 ps. The time delay increases from left to right.

3.3 Two-colour experiments in one shot

To address the fundamental question in element-sensitive pump-probe experiments whether a compound material of two different elements exhibits similar dynamcis for each of the contained elements, we employed the specifically developed zone plate for two energies $\frac{E_1}{E_2} = \frac{13}{11}$, as described in Section 2.3. The fixed ratio of these two energies is due to the use of two harmonics of the seed laser of the FERMI FEL. This setup allows to maintain the absolute relation in the timing of pump and the two probe beams. Figure 9 shows the projection of the zone plate illumination onto the CCD detector. In order to relate the different diffraction orders, we mounted a lithographically patterned chromium mask in front of the zone plate, acting as a shadow mask.

The image depicts the projection of the pathways which meet in the split focus spot on the sample (the yellow dots in Figure 5). Each of the halves of the optical elements is energy-specific. On the detector image, the weaker part represents 53.5 eV (more attenuated by an aluminum filter upstream), whereas the stronger intensity represents 63.2 eV. The focus point on the sample of the upper projection is later on pumped, whereas the lower part remains unpumped and can be used for normalization.

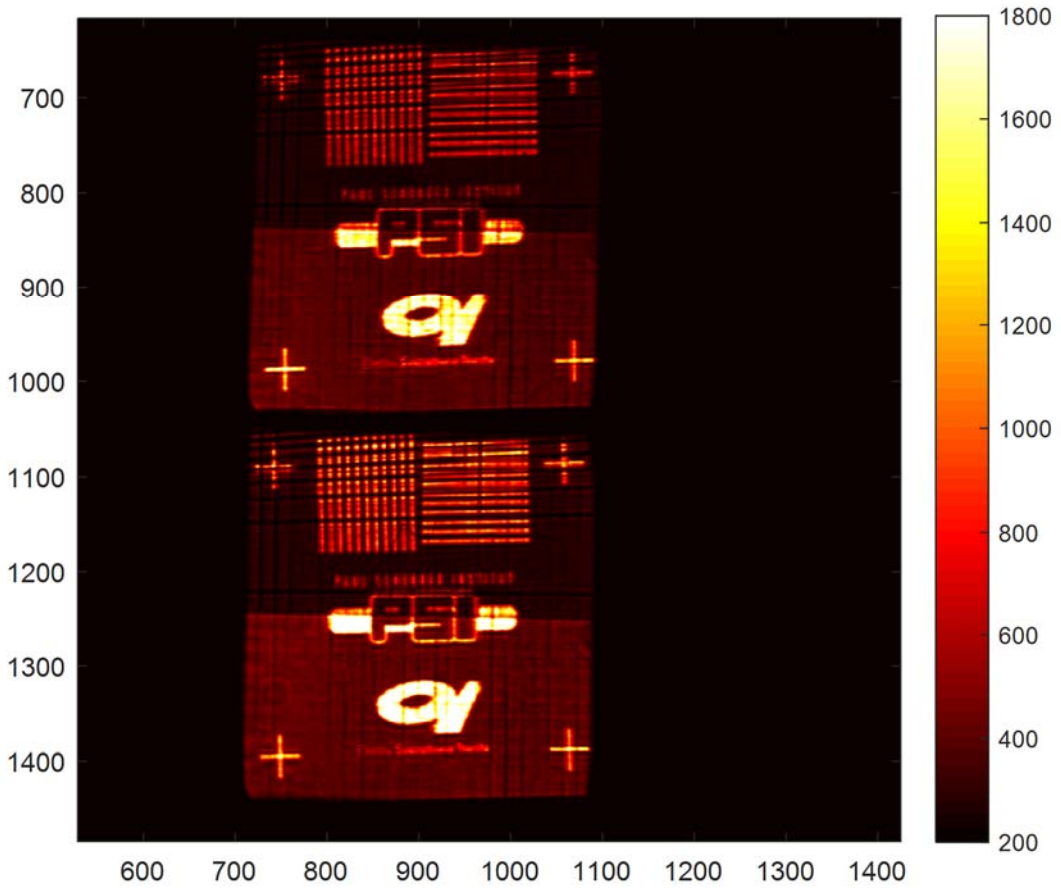

Figure 9 – Projection of the two energies and two focal spots onto the CCD detector. The upper parts with the line grating are arising from the beam with 53.5 eV, the lower parts of the projection with the Elettra logo from 63.2 eV. The focus spot of the upper projection is pumped on the sample, whereas the area remains unpumped where the beam of the lower projection passes the sample. The lines, crosses and logos are product of a chromium shadow mask mounted in front of the zone plate to illuminate it in an inhomogeneous fashion to be able to track the different diffraction orders and pathways of the radiation.

4. Conclusions

The demonstration of the possibilities to conduct pump-probe experiments in one single shot is expected to have major impact in the community. Especially for X-ray FELs, this enables to investigate material systems which were not accessible before due to degradation by the extremely high photon densities of an FEL, or because the systems are not restored in time.

Especially the concept to use two energies at the same time tackles a major issue which is up to now inherent to pump-probe experiments. Whenever the energy is changed, even in a fixed geometry, the information on absolute time delay between pump and probe is lost. Whereas dynamics can be obtained for at two probe energies independently, their time zero (i.e., the time when an observed effects sets effectively in) cannot be related. With the newly developed concept, we are able to avoid this problem by probing simultaneously with the two different energies. The fixed geometry of both energies ensures that both the time window and the absolute timing are the same. This will open a wide range of possibilites to investigate which element is responsible for a certain effect in alloys, mixtures or compound materials.

References

[1] *C. David et al., Sci. Rep.* ***5****, 7644 (2015).*
[2] *M. Buzzi et al., Sci. Rep.* ***7****, 7235 (2017).*
[3] *Vinko, S. M. et al., Nature* ***482****, 59–63 (2012).*
[4] *Glownia, J. M. et al., Opt. Express* ***18****, 17620–17630 (2010).*
[5] *Tavella, F. et al., Nature Photon.* ***5****, 162–165 (2011).*
[6] *Löhl, F. et al., Phys. Rev. Lett.* ***104****, 144801 (2010).*
[7] *Harmand, M. et al., Nature Phot.* ***7****, 215–218 (2013).*
[8] *Sorgenfrei, F. et al., Rev. Sci. Instrum.* ***81****, 043107–7 (2010).*
[9] *Castagna, J. C. et al., J. Phys.: Conf. Ser.* ***425****, 152021–5 (2013).*
[10] *Roseker, W. et al., Opt. Lett.* ***34****, 1768–1770 (2009).*
[11] *Roseker, W. et al., J. Synchrotron Rad.* ***18****, 481–491 (2011).*